

UNCLASSIFIED
AD 432831

DEFENSE DOCUMENTATION CENTER
FOR
SCIENTIFIC AND TECHNICAL INFORMATION
CAMERON STATION, ALEXANDRIA, VIRGINIA



UNCLASSIFIED

NOTICE: When government or other drawings, specifications or other data are used for any purpose other than in connection with a definitely related government procurement operation, the U. S. Government thereby incurs no responsibility, nor any obligation whatsoever; and the fact that the Government may have formulated, furnished, or in any way supplied the said drawings, specifications, or other data is not to be regarded by implication or otherwise as in any manner licensing the holder or any other person or corporation, or conveying any rights or permission to manufacture, use or sell any patented invention that may in any way be related thereto.

AEDC-TDR-64-14

432831



CATALOGED BY DDC

432831

INVESTIGATION OF FLOW SEPARATION
ON A TWO-DIMENSIONAL FLAT PLATE
HAVING A VARIABLE-SPAN TRAILING-
EDGE FLAP AT $M_{\infty} = 3$ AND 5

By

S. R. Pate

von Kármán Gas Dynamics Facility

ARO, Inc.

TECHNICAL DOCUMENTARY REPORT NO. AEDC-TDR-64-14

March 1964

Program Element 64406124/627A

(Prepared under Contract No. AF 40(600)-1000 by ARO, Inc.,
contract operator of AEDC, Arnold Air Force Station, Tenn.)

ARNOLD ENGINEERING DEVELOPMENT CENTER
AIR FORCE SYSTEMS COMMAND
UNITED STATES AIR FORCE

NOTICES

Qualified requesters may obtain copies of this report from DJC, Cameron Station, Alexandria, Va. Orders will be expedited if placed through the librarian or other staff member designated to request and receive documents from DDC.

When Government drawings, specifications or other data are used for any purpose other than in connection with a definitely related Government procurement operation, the United States Government thereby incurs no responsibility nor any obligation whatsoever; and the fact that the Government may have formulated, furnished, or in any way supplied the said drawings, specifications, or other data, is not to be regarded by implication or otherwise as in any manner licensing the holder or any other person or corporation, or conveying any rights or permission to manufacture, use, or sell any patented invention that may in any way be related thereto.

INVESTIGATION OF FLOW SEPARATION
ON A TWO-DIMENSIONAL FLAT PLATE
HAVING A VARIABLE-SPAN TRAILING-
EDGE FLAP AT $M_\infty = 3$ AND 5

By

S. R. Pate

von Kármán Gas Dynamics Facility

ARO, Inc.

a subsidiary of Sverdrup and Parcel, Inc.

March 1964

ARO Project VD0350

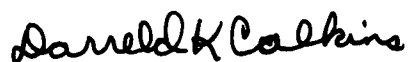
ABSTRACT

An experimental investigation of separated boundary-layer flow was conducted on a two-dimensional flat plate having a variable-span trailing-edge flap in the 12-in. Supersonic Tunnel (D) of the von Kármán Gas Dynamics Facility. The tests were made at Mach numbers 3 and 5 at zero angle of attack and over a Reynolds number range (based on plate length) from 0.26 to 16.7×10^6 .

Model surface pressure distributions, schlieren photographs, and velocity distributions are presented. The effects of unit Reynolds number, plate length, flap span, and flap deflection angle on the separated region are investigated, and comparisons are made with existing theory.

PUBLICATION REVIEW

This report has been reviewed and publication is approved.



Darreld K. Calkins
Major, USAF
AF Representative, VKF
DCS/Test



Jean A. Jack
Colonel, USAF
DCS/Test

CONTENTS

	<u>Page</u>
ABSTRACT	iii
NOMENCLATURE	viii
1.0 INTRODUCTION	1
2.0 APPARATUS	
2.1 Wind Tunnel	1
2.2 Model	2
2.3 Boundary-Layer Probe	2
2.4 Instrumentation	3
3.0 TEST PROCEDURE	3
4.0 RESULTS AND DISCUSSION	
4.1 Transition Results for Zero Flap Deflection	4
4.2 Separation Results for $M_\infty = 3$, 8-in. Plate	5
4.3 Separation Results for $M_\infty = 3$, 20-in. Plate	8
4.4 Separation Results for $M_\infty = 5$, 8- and 20-in. Plates	8
4.5 Comparisons between the Experimental Data and Existing Semi-Empirical Results	9
5.0 CONCLUDING REMARKS	11
REFERENCES	12

ILLUSTRATIONS

<u>Figure</u>	
1. Tunnel D	15
2. Model Photographs	
a. Model	16
b. Model Installation	16
3. Model Geometry	17
4. Boundary-Layer Transition Results at $M_\infty = 3$ and 5 for Zero Flap Deflection	
a. $M_\infty = 3$, Schlieren and Sublimable Solid Results	18
b. $M_\infty = 5$, Schlieren Results	18
5. Velocity Profiles and Boundary-Layer Thickness at Various Model Stations, $M_\infty = 3$, $\theta = 0$	
a. Velocity Profiles at Various Model Stations	19
b. Boundary-Layer Growth	19

<u>Figure</u>	<u>Page</u>
6. Velocity Distributions and Surface Pressure Distribution at $M_\infty = 3$, $Re/in. = 0.036 \times 10^6$, $\theta = 30$ deg, Configuration 839	
a. Schlieren Photograph	20
b. Flow Model	20
c. Velocity Profiles (u/U_∞)	20
d. Pressure Distribution.	20
7. Effect of Unit Reynolds Number on Surface Pressure Distribution and Separation, 8-in. Plate, $M_\infty = 3$, Configuration 839	
a. $\theta = 30$ deg	21
b. $\theta = 10$ deg	22
8. Flap Span and Unit Reynolds Number Effect, 8-in. Plate, $M_\infty = 3$	
a. Flap Span Effect, $\theta = 30$ deg, $Re/in. \approx 0.034 \times 10^6$	23
b. Flap Span Effect, $\theta = 20$ deg, $Re/in. = 0.095 \times 10^6$	24
c. Flap Span and Reynolds Number Effect, $\theta = 30$ and 20 deg.	25
9. Comparison of Separation Locations for Various Flap Angles and Flap Span Widths, 8-in. Plate, $M_\infty = 3$	26
10. The Effect of Flap Span and Unit Reynolds Number for $M_\infty = 3$, $\theta = 30$ and 20 deg, Configurations 2033 and 2039	27
11. The Effect of Unit Reynolds Number, 8-in. Plate, $M_\infty = 5$, Configuration 839	
a. $\theta = 30$ deg	28
b. $\theta = 15$ deg	29
12. Variation in Separation Locations with Flap Deflection Angle (θ) at $M_\infty = 5$	
a. 8-in. Plate	30
b. 20-in. Plate	31
13. Plateau Pressure for Laminar and Transitional Flow	
a. $M_\infty = 1$ to 7	32
b. $M_\infty = 3$	32
c. $M_\infty = 5$	32

<u>Figure</u>	<u>Page</u>
14. Length of Laminar and Transitional Separation . .	33
15. Variation in Separation Location with Flap Deflection Angle (θ), $M_\infty = 3$, Configuration 839. .	34

NOMENCLATURE

b	Model leading edge thickness, in.
C_{pp}	Plateau pressure coefficient, $(p_p - p_\infty)/q_\infty$
h	Probe height, in.
l_s	Length of separated region, in. (see Fig. 6)
M_∞	Free-stream Mach number
p	Surface pressure, psia
p_F	Final flap pressure (see Fig. 6d), psia
p_p	Plateau pressure, psia
p_∞	Free-stream static pressure, psia
q_∞	Free-stream dynamic pressure, psia
R	Reattachment point of separated region
Re/in.	Reynolds number per inch, U_∞/ν_∞
Re_t	Reynolds number based on distance from model leading edge to transition, $U_\infty x_t/\nu_\infty$
Re_{x_0}	Reynolds number based on distance from model leading edge to interaction region, $U_\infty x_0/\nu_\infty$
S	Surface distance, in.
Sep.	Point of boundary-layer separation
U_∞	Free-stream velocity, in./sec
u	Velocity in boundary layer or separated region, in./sec
x	Distance from model leading edge, in.
x_0	Distance from model leading edge to beginning of interaction region, in.
x_s	Distance from model leading edge to separation, in.
x_t	Boundary layer transition location, in.
y	Distance perpendicular to plate surface, in.
σ	Flow deflection angle, deg
β	Model leading edge included angle, deg
δ	Boundary layer total thickness, in.
δ_0	Undisturbed boundary layer total thickness at x_0 , in.
ν_∞	Free-stream kinematic viscosity, in. ² /sec
θ	Flap deflection angle, deg

1.0 INTRODUCTION

At the request of the Ballistic Systems Division (BSD), Air Force Systems Command (AFSC), an experimental investigation of boundary-layer separation on a flat plate with a variable-span trailing-edge flap was conducted for the Space Technology Center of the General Electric Company. Tests were made in the Gas Dynamic Wind Tunnel, Supersonic (D) of the von Kármán Gas Dynamics Facility (VKF), Arnold Engineering Development Center (AEDC), during the period from June 3 to July 27, 1963. Test Mach numbers were 3 and 5, the Reynolds number range (based on model plate length) was from 0.26 to 16.7×10^6 , the model angle of attack was zero, and flap deflection angle was varied from 7.5 to 30 deg.

This investigation was designed to provide basic flow separation data (i. e., separation occurring when the momentum of the viscous-layer flow is unable to overcome the adverse pressure gradient that is imposed by the deflected flap) on a 12-in. -wide flat plate of variable length (8 and 20 in.), with a variable-span (3, 6, and 9 in.) trailing-edge flap.

Most of the basic separation data published to date pertains to either fully laminar or fully turbulent flow (boundary-layer tripped), and only a limited amount of data is available for flows where transition occurs near reattachment.

This investigation provided separation data on fully laminar flow (transition downstream of flow reattachment), transitional flow (transition between reattachment and separation), and fully turbulent flow (transition upstream of separation) with transition occurring naturally. Most of the data presented is for transitional type separation where transition moves forward with increasing Reynolds number from a position downstream of reattachment to a position upstream of separation and hence fully turbulent flow.

2.0 APPARATUS

2.1 WIND TUNNEL

The 12- x 12-in. Supersonic Tunnel (D) (Fig. 1) is an intermittent, variable density wind tunnel with a manually adjusted, flexible plate-type nozzle. The tunnel operates at Mach numbers from 1.5 to 5 at stagnation

Manuscript received January 1964.

pressures from about 5 to 60 psia and at stagnation temperatures up to about 100°F. A description of the tunnel and its calibration are given in Refs. 1 and 2.

2.2 MODEL

The model (Figs. 2 and 3) was supplied by the General Electric Company and consisted of a 12-in. -wide rectangular flat plate with a removable middle section, detachable leading edge, and a variable-span trailing-edge flap. Removal of the middle plate section (see Fig. 3) enabled the plate length to be changed from 20 to 8 in. The plate was strut-mounted as shown in Fig. 2b and had a rubber "O" ring insert between the model and tunnel wall to prevent bleed of flow from high pressure regions on the underside of the plate. The flap span was variable to 3, 6, and 9 in., and flap chord lengths of 3 and 4 in. were provided. The 3-in. span was the primary flap arrangement, and the 6- and 9-in. span flaps were obtained by adding sections to the 3-in. span (see Fig. 2a). The 6- and 9-in. spans were always deflected as a solid span, i. e., the complete flap acted as a common unit ($\theta = \text{constant}$). The 4-in. chord length was obtained by adding a 1-in. extension to the 3-in. chord (Fig. 2a) and was only used when the flap chord extension was required to obtain the full pressure rise in cases where the separated boundary-layer reattachment occurred close to the tip of the 3-in. chord. Flap deflection was obtained by jack screws mounted on a support plate and connected to the individual span sections (Fig. 3). The jack support plate also helped prevent the high pressure air beneath the model from influencing flow over the flap.

When the 3- or 6-in. span flap was being tested, the outboard flap sections were removed from the model so that the conditions which exist for a trailing flap could be more accurately simulated. The model leading edge had an included angle (β) of 12 deg and a leading edge thickness that varied randomly across the width from 0.004 to 0.006 in.

2.3 BOUNDARY-LAYER PROBE

A pitot probe was employed to survey the boundary layer and separated flow regions. Surveys could be made at eleven different stations along the plate, 0.5 in. off model centerline (see Table, Fig. 3). The probe shaft passed through the flat plate and was connected to a probe drive mechanism located under the model which was operated manually from outside the tunnel. The height of the probe above the model plate surface could be varied from zero to 1.0 in. with an accuracy of ± 0.002 in.

Probe height was determined by a calibrated counter that was connected to the probe drive shaft. The probe tip was approximately elliptical, with inside dimensions of 0.017 and 0.030 in., as shown in Fig. 3.

2.4 INSTRUMENTATION

The model was instrumented to measure 44 surface centerline pressures (18 on flap), 9 pressures located 1 in. off centerline (3 on flap), and 9 pressures located 2 in. off centerline (3 on flap). All surface pressure orifice diameters were 0.020 in. Four copper-constantan thermocouples were also located on the model surface 0.5 in. off centerline. (See the table in Fig. 3 for specific locations of the pressure orifices and thermocouples). Model pressures were measured with a sequential pressure switching system having eight synchronized valves, each valve being independently connected to a 1- and 15-psid transducer with a near vacuum reference. The 1-psid transducers were calibrated for ranges of 0.15, 0.50, and 1.0 psia, and the 15-psid transducers for 3, 7, and 15 psia. The precision of this system is estimated to be ± 0.5 percent of the range being used for the pressure measurement. Transducer outputs were visually monitored, and the instrument sensitivities for measurement of model pressures to the best available precision were manually selected.

3.0 TEST PROCEDURE

Testing was conducted at the following nominal conditions.

Configuration	M_∞	θ , deg	Re/in. $\times 10^{-6}$	
			Min	Max
833, 843*	3	0, 7.5, 10, 20, 30	0.033	0.82
836, 846*	3	7.5, 10, 20, 30	0.032	0.83
839, 849*	3	0**, 7.5, 10**, 20, 30**	0.034	0.84
2033	3	10**, 20, 25, 30	0.034	0.83
2036	3	20, 30	0.033	0.81
2039	3	0**, 10, 15, 20, 25, 30	0.033	0.79
843*	5	7.5, 10, 20	0.049	0.28
846*	5	7.5, 10, 20	0.094	0.29
839, 849*	5	7.5, 10, 15, 20, 30	0.093	0.30
2036	5	20, 25, 30	0.048	0.28
2039	5	10, 20, 30	0.047	0.28

*Indicates only schlieren data obtained

**Indicates probe data obtained

Configuration Code: Example: 833 - 8-in. plate
 3-in. chord
 3-in. flap span
 2039 - 20-in. plate
 3-in. chord
 9-in. flap span

Boundary-layer transition was determined from schlieren photographs and by a sublimable solid technique, as described in Ref. 3.

4.0 RESULTS AND DISCUSSION

4.1 TRANSITION RESULTS FOR ZERO FLAP DEFLECTION

Presented in Fig. 4 are the boundary layer transition results for $M_\infty = 3$ and 5, as determined from schlieren photographs and visually by the sublimable solid technique. Each schlieren data point presented was obtained from a single photograph, although the better method would be to average the results from many photographs and thereby eliminate some of the uncertainty in reading the photographs. The purpose of this study was not to investigate transition for $\theta = 0$, since this has been done by Potter and Whitfield (Ref. 4), but only to verify that transition was not occurring prematurely. The transition Reynolds number results as determined from a correlation based on the leading edge geometry (b, β) by Potter and Whitfield (Ref. 4) for $M_\infty = 3$ are presented in Fig. 4a for $b = 0.004$ in., $\beta = 12$ deg and $b = 0.006$ in., $\beta = 12$ deg and are in good agreement with the present experimental data at $Re/in. < 0.3 \times 10^6$. At a sufficiently high unit Reynolds number, the transition Reynolds number results of Ref. 4 deviated from the correlation predictions, as do the transition results presented in Fig. 4a. The determination of boundary-layer transition locations depends upon the methods used, with the transition Reynolds number determined from schlieren photographs being slightly less than the one determined from hot wire results. The Potter-Whitfield correlation was based on hot wire measurements, and their results were arbitrarily reduced 10 percent to give a more valid comparison with the present schlieren results [$Re_t = (0.9)(Re_t)_{hot\ wire}$].

The velocity profiles obtained with the pitot probe are presented in Fig. 5a for $M_\infty = 3$ at three unit Reynolds numbers and for model stations 4.5, 11.5, and 18.5 in. from the leading edge. At station $x = 4.5$ in. the velocity profiles show that the flow was laminar up through $Re/in. = 0.41 \times 10^6$, but at station $x = 11.5$ and 18.5 in. transition from laminar to turbulent flow occurred between $Re/in. = 0.034$ and 0.14×10^6 .

Figure 5b presents the boundary-layer growth (total thickness, δ) for $M_\infty = 3$, $\theta = 0$ from $x = 4.5$ to 18.5 in. over the unit Reynolds number range from 0.034 to 0.54×10^6 . As seen from these data and defining transition location as the point where $d\delta/dx$ deviates from the

laminar flow trend, laminar flow existed up to $x = 18.5$ in. for $Re/in. = 0.034 \times 10^6$ and up to $x = 11.5$ in. for $Re/in. \leq 0.095$. For $Re/in. = 0.14 \times 10^6$ transition occurred at approximately $x = 9.5$ in. and decreased with increasing unit Reynolds number. For comparative purposes, the transition locations as determined from the schlieren results (Fig. 4a) are also presented in Fig. 5b.

The data in Fig. 5 were presented with the intention only of indicating the state of boundary-layer flow on the flat plate for the conditions of the test and are not necessarily an accurate measurement of boundary-layer thickness, especially for the laminar boundary layers. For most of the laminar data the ratio of probe height to boundary-layer thickness (h/δ) was greater than the value 0.20 to 0.29, which has been shown to be a critical factor in obtaining accurate velocity profile measurements with a pitot probe (Refs. 5, 6, and 7). Also, the laminar skin friction values determined from the experimental velocity profiles were higher than the theoretical values and showed that the experimental skin friction values were dependent on the h/δ value, as has also been shown by Blue (Ref. 7) to be the result of probe size.

4.2 SEPARATION RESULTS FOR $M_\infty = 3$, 8-IN. PLATE

In the following discussions on the flow separation results, the point of flow separation (x_s) is defined as the location where the boundary layer deviates from the plate surface as determined from schlieren photographs, and this is in general agreement with the location determined by extending the shock generated by flow separation (after coalescence) back to the model surface. Other definitions used consistently during this discussion are the distance (x_0) from the model leading edge to the point where p/p_∞ deviates from unity and δ_0 , the boundary-layer thickness at x_0 . The definitions (x_s , x_0 , δ_0) as applied to the experimental data are shown in Fig. 6.

Presented in Fig. 6 are schlieren, velocity distribution profiles, and pressure distribution data obtained for configuration 839 with flow separation occurring at $M_\infty = 3$, $Re/in. = 0.036 \times 10^6$, and for a flap deflection angle of 30 deg. The sketch of the flow model presented in Fig. 6b was determined from the schlieren photograph in Fig. 6a. Shown in Fig. 6c are the velocity profiles obtained at three stations superimposed on a sketch of the separated boundary layer. The pitot probe was used as a forward- and rearward-facing probe in the separated region. These profiles allow an approximation to be made of the location of the dividing streamline ($u = 0$), which here appears to be

parallel to the underside of the separated boundary layer. The velocity profile measured in the boundary layer at station $S = 6.5$ in. is similar to a laminar profile, which is not unexpected since transition (as indicated by the schlieren, Fig. 6a) occurs downstream of this position. The velocities in the separated region decrease as the distance forward of the flap hinge line ($S = 8$ in.) increases.

The pressure distribution data obtained along the model centerline and 2 in. off centerline are presented in Fig. 6d and show that the flow separation along the model centerline for this flap configuration can be considered two-dimensional. Also presented in Fig. 6d are the theoretical pressure distributions resulting from the inviscid results $[p/p_\infty = f(M_\infty, \theta)]$ and the idealized viscous results $[p/p_\infty = f(M_\infty, \sigma, \theta)]$ in which the separated region is assumed to act as a simple compression surface having a constant flow deflection angle, σ (measured from schlieren photograph, Fig. 6a). It is seen that the idealized viscous pressure distributions are in good agreement with the experimental plateau (p_P) and final flap pressure (p_F).

The separated flow in Fig. 6 is a transitional-type flow separation because transition occurs slightly upstream of flow reattachment, as seen in Fig. 6a. One characteristic of transitional-type flow separation, where transition occurs near reattachment (Ref. 8), is the rapid increase in pressure upstream of the reattachment zone, as is seen to exist in Fig. 6d.

The effect of increasing the unit Reynolds number is shown in Fig. 7 for $M_\infty = 3$, configuration 839, and $\theta = 30$ and 10 deg. From Figs. 6 and 7a, the separation results for $\theta = 30$ deg show that when the free-stream unit Reynolds number was increased from $Re/in. = 0.036$ to 0.42×10^6 , transition (x_t) moved forward from near the reattachment point until transition occurred upstream of the separated region. As seen from these data, there was a surface pressure increase associated with transition when transition occurred between reattachment and separation. As $Re/in.$ was increased there was a decrease in the length of separation (l_S , see Fig. 6b) until fully turbulent flow and turbulent separation were obtained. A short plateau region existed for $Re/in. = 0.097 \times 10^6$, but a plateau was not discernible for $Re/in. = 0.21$ and 0.28×10^6 . Figure 7b presents the effects of unit Reynolds number for a flap deflection angle (θ) of 10 deg. The flow is two-dimensional as indicated by the pressures on and off centerline. These data are similar to the previous $\theta = 30$ deg data in that an increase in $Re/in.$ decreased the length of separation. For $Re/in. = 0.034 \times 10^6$ the flow appears to be fully laminar. At $Re/in. = 0.094 \times 10^6$ transition occurred in the

region of flow reattachment and the result was a shorter separation length, but for $Re/in. = 0.26 \times 10^6$ transition was upstream of the flap and the 10-deg flap deflection did not produce any notable separation in the fully turbulent flow. There was also the small increase in final flap pressure as the unit Reynolds number was increased.

The effect of flap span (8-in. plate) on separation distance and surface pressure distribution is presented in Fig. 8 for $M_\infty = 3$ and $\theta = 30$ and 20 deg. For each trailing-edge flap deflection and transition occurring near reattachment (Figs. 8a and b) a well-defined plateau pressure exists. The effect of decreasing the flap span was a decrease in the separation length and plateau pressure. The pressure distribution for the 6-in. span flap (configuration 836) appears to be approximately two-dimensional in nature, since the pressure data on centerline and 2 in. off centerline indicate no significant difference, but the separation distance as compared to the 9-in. span flap decreased slightly. The pressures on the flap on the 3-in. span (configuration 833) 1.0 in. off centerline show a definite span effect because of the sizeable reduction in pressure. Also the separation distance decreases considerably with the 3-in. span as compared to the 9-in. span. It should be noted that the plate spanwise surface pressure upstream of the 3-in. span flap was essentially the same on centerline and 1 in. off centerline, indicating that the separated region upstream of the flap hingeline was of a more uniform width than would be deduced from observing the flap pressures.

Figure 8c shows the effect of flap span and flap deflection angle (θ) as the unit Reynolds number is increased and the flow changed from transitional to fully turbulent. A flap angle (θ) of 30 deg for configurations 839 and 833 was sufficient to cause turbulent separation up to the maximum available unit Reynolds number of $Re/in. \approx 0.84 \times 10^6$. The three-dimensional effect resulting from the 3-in. span flap (configuration 833) is evident from the flap pressure distribution and similar to the previous results. The turbulent separated flow region for the 3-in. span flap was also smaller than that for the 9-in. span flap ($Re/in. \approx 0.42$ and 0.84×10^6). For $\theta = 20$ deg, $Re/in. = 0.33 \times 10^6$, and turbulent flow, no separation existed for configuration 839.

A summary plot is presented in Fig. 9 for the separation locations obtained on configurations 839 and 833 as determined from schlieren photographs for $M_\infty = 3$ and $\theta = 75, 10, 20,$ and 30 deg, over the unit Reynolds number range from $Re/in. = 0.032$ to 0.84×10^6 . For both configurations the distance from the model leading edge to separation, x_s , increased with increasing unit Reynolds number until the flow became turbulent, and no separation (based on earlier definition) occurred

for $\theta \leq 20$ deg. For $\theta = 30$ deg, turbulent separation occurred above $Re/in. \approx 0.4 \times 10^6$ for both configurations. Decreasing the flap deflection angle of course reduced the separation length, l_s , considerably. The trends exhibited by both configurations are seen to be very similar, with the length of the separated region resulting from the 9-in. span flap (configuration 839) being significantly longer than the 3-in. span flap (configuration 833), as has been shown previously.

4.3 SEPARATION RESULTS FOR $M_\infty = 3$, 20-IN. PLATE

Presented in Fig. 10 are the separation results for configurations 2033 and 2039 at $M_\infty = 3$, $\theta = 30$ and 20 deg for a unit Reynolds number range from 0.034 to 0.81×10^6 . Transitional-type separation occurred for both deflection angles at $Re/in. = 0.034 \times 10^6$, but as the unit Reynolds number was increased from 0.034 to 0.053×10^6 , transition moved upstream of separation and fully turbulent separated flow occurred for $\theta = 30$ deg, but no separation occurred for $\theta = 20$ deg. The 3-in. span flap exhibited the usual decrease in flap pressure with distance from centerline and had the familiar smaller separated region than the 9-in. span flap. Increasing the unit Reynolds number after turbulent separation occurred moved the point of separation (x_s , as determined from schlieren photographs) forward for the 3-in. and 9-in. span flap, but did not affect the no-separation condition at $\theta = 20$ deg.

The trend of the turbulent separated flow data for both the 8-in. plate (Fig. 8c) and 20-in. plate (Fig. 10) has shown that after turbulent separation occurred for $\theta = 30$ deg, the effect of increasing the unit Reynolds number appears to be an increase in the length of the separation region. This trend is in agreement with results of Ref. 8 and in general agreement with Kuehn's results (Ref. 9).

4.4 SEPARATION RESULTS FOR $M_\infty = 5$, 8- AND 20-IN. PLATES

The effect of unit Reynolds number at $M_\infty = 5$ is presented in Fig. 11 for configuration 839 and $\theta = 30$ and 15 deg. Over the unit Reynolds number range $Re/in. = 0.097$ to 0.30×10^6 at $\theta = 7.5$ deg (Fig. 11a), there was only a small Reynolds number effect on the length of the separated region. There was also a small decrease in the plateau pressure as the unit Reynolds number increased. The theoretical idealized viscous results $[p/p_\infty = f(M_\infty, \sigma, \theta)]$ give good agreement with the experimental plateau and final flap pressures (p_F/p_∞). It is of interest to note that the final flap pressure as determined by applying the inviscid flow

relation $[p/p_\infty = f(M_\infty, \theta)]$ differs considerably from the results obtained experimentally and from the idealized viscous results. The transition location did not move upstream from the reattachment point as the unit Reynolds number was increased as was the case for the $M_\infty = 3$ data, but remained near the reattachment point up to the maximum obtainable unit Reynolds number of 0.30×10^6 . The small effect of unit Reynolds number on the length of the separated region is believed to be the direct result of transition remaining near the reattachment point.

The results for $\theta = 15$ deg are presented in Fig. 11b and are similar to the $\theta = 30$ deg results in that increasing the unit Reynolds number decreased the plateau pressure but had little effect on the length of the separated flow.

The locations for the point of flow separation and reattachment as determined from schlieren photographs at $M_\infty = 5$ on the 8-in. plate are shown in Fig. 12a for $\theta = 7.5, 10, 15, 20,$ and 30 deg over the unit Reynolds number range from $Re/in. \approx 0.048$ to $\approx 0.29 \times 10^6$ for configurations 839, 849, 846, and 843. The effect of unit Reynolds number on length of flow separation was insignificant, and the length of flow separation decreased with decreasing flap span and decreasing flap deflection angle (θ), while the reattachment point remained relatively constant and independent of flap span and flap deflection angle. The reattachment point being independent of flap deflection angle (θ) was also observed in Ref. 10.

A summary of the separation locations, x_s , for the 20-in. plate (configurations 2036 and 2039) at $M_\infty = 5$ is shown in Fig. 12b for $\theta = 10$ to 30 deg and a unit Reynolds number range from ≈ 0.048 to $\approx 0.28 \times 10^6$. Schlieren photographs of configuration 2039 at various unit Reynolds numbers and $\theta = 20$ deg are also presented.

4.5 COMPARISONS BETWEEN THE EXPERIMENTAL DATA AND EXISTING SEMI-EMPIRICAL RESULTS

Chapman, Kuehn, and Larson (Ref. 8) have shown that an order-of-magnitude analysis of free interaction for laminar flow gives the relation $C_{pP} \sim (R_{x0})^{-1/4}$. Erdos and Pallone (Ref. 11) have also derived the relation $C_{pP} = A (R_{x0})^{-1/4}$, where A is a function of free-stream Mach number. Presented in Fig. 13a are some experimental plateau pressure coefficients (C_{pP}) for transitional and laminar flow separation at $M_\infty = 3$ and 5 , configuration 839, obtained in the VKF-AEDC investigation. Also shown are other experimental data presented

in Ref. 11 and the Erdos and Pallone (Ref. 11) semi-empirical laminar flow results. Good agreement exists at $M_\infty = 3$ between the theoretically predicted and the VKF - AEDC experimental laminar flow plateau pressure coefficients. At Mach numbers 3 and 5 the transitional separation plateau pressure coefficients were higher than the laminar values. Although transition occurred in the reattachment region for the VKF - AEDC, $M_\infty = 5$, $\theta = 15$ data, the trend of the previous flap data (Refs. 8, 14, 12) and the present flap data indicate that the results of Erdos and Pallone (Ref. 11) might not give as good agreement for flaps as compared to forward facing steps at the higher Mach numbers.

A correlation of the plateau pressure coefficients for $M_\infty = 3$ is presented in Fig. 13b. The data are for $\theta = 7.5, 10, 20,$ and 30 deg, configurations 839, 836, and 833, and various values of free-stream unit Reynolds number. As seen from the figure, there is no difference between the correlation where transition occurs in the reattachment zone and where transition occurs upstream of reattachment. The pure laminar separation plateau pressure coefficient is in good agreement with the semi-empirical results of Erdos and Pallone (Ref. 11), but the transitional-type flow separation data are appreciably higher than the laminar flow results. The transitional-type data follow the correlation $C_{pP} \sim (Re_{x0})^{-1/4}$ for $Re_{x0} < 0.25 \times 10^6$, but as Re_{x0} increases the pressure coefficient decreases. This decrease in C_{pP} is explained by observing Fig. 7a and noting that as $Re/in.$ increases and consequently Re_{x0} increases, C_{pP} decreases. This leads to the conclusion that the correlation $C_{pP} \sim (Re_{x0})^{-1/4}$ is only valid for pure laminar separation and transitional-type flow where a well defined plateau exists and transition is relatively near reattachment.

The correlation of the $M_\infty = 5$ plateau pressure coefficients is presented in Fig. 13c and follows the same pattern as exhibited by the $M_\infty = 3$ correlation results.

Erdos and Pallone (Ref. 11) developed the relation $\frac{l_{sep.}}{\delta_0} = \left(\frac{l_{sep.}}{\delta_0}\right)_{ref.} \left(\frac{\sigma_{ref.}}{\sigma}\right)$ where $\left(\frac{l_{sep.}}{\delta_0}\right)_{ref.}$ is for the condition of a free-interaction separated flow. Correlation of $\left(\frac{l_{sep.}}{\delta_0}\right)_{ref.}$ from the data of Ref. 12 as determined by Erdos and Pallone are presented in Fig. 14. The results from the present VKF $M_\infty = 3$ (configuration 839) data as determined by $\left(\frac{l_{sep.}}{\delta_0}\right)_{ref.} = \left(\frac{\sigma}{\sigma_{ref.}}\right) \left(\frac{l_{sep.}}{\delta_0}\right)$ (where $\sigma_{ref.} = 2.7$ deg) is seen to be in excellent agreement with the Ref. 12 data for $\theta = 7.5$ and 10 deg and a unit Reynolds number of 0.034×10^6 . At $\theta = 20$ and 30 deg, $Re/in. = 0.034 \times 10^6$,

the present data give correlation results lower than would be obtained by an extrapolation of the transitional results of Erdos and Pallone. The separation data of Ref. 12 was on a flat plate utilizing an incident shock to produce the pressure rise to cause separation. The transition location has a pronounced effect on the correlation, as seen by comparing the data for $Re/in. = 0.034$ and 0.095×10^6 where transition moved farther upstream from reattachment with increasing $Re/in.$ For comparative purposes only, the turbulent correlation results ($\sigma_{ref.} = 12.4$ deg) from Erdos and Pallone (Ref. 11) are also presented.

Using the results of Erdos and Pallone (Ref. 11), the fully laminar and fully turbulent separation locations can be predicted. Figure 15 presents a comparison of the VKF Mach 3 experimental data with the predictions of Erdos and Pallone. The data for $\theta = 7.5$ deg, $Re/in. = 0.034 \times 10^6$ is in excellent agreement with the predicted fully laminar separation locations. The turbulent separation predictions give the same slope as the experimental data but give longer lengths of separation.

5.0 CONCLUDING REMARKS

Tests were conducted at Mach numbers 3 and 5 over the Reynolds number range (based on plate length) from 0.26 to 16.7×10^6 to investigate the effects of a variable-span trailing-edge flap on boundary-layer separation. Based on these investigations the following conclusions are made:

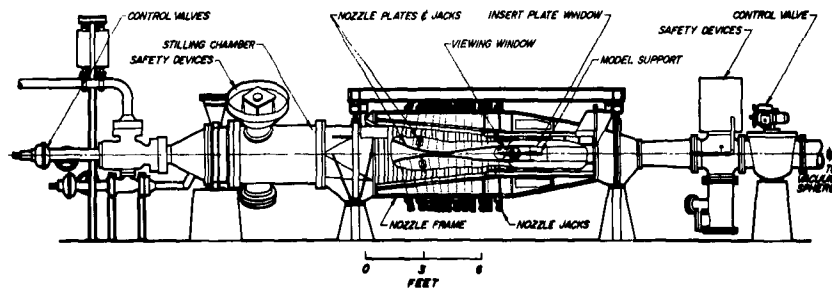
1. For $M_\infty = 3$, increasing the unit Reynolds number decreased the length of flow separation. At $M_\infty = 5$ on the 8-in. plate, increasing the unit Reynolds number had a negligible effect in the transition location and on the length of separation. At $M_\infty = 5$ on the 20-in. plate, increasing unit Reynolds number decreased the length of flow separation. At $M_\infty = 3$ and transition occurring between the point of reattachment and flow separation, there was an accompanying rise in model surface pressures in the region of transition. At $M_\infty = 3$ and a flap deflection angle of 30 deg, turbulent separation occurred, but for $\theta \leq 20$ deg no separation was obtained.
2. Increasing the flap deflection angle increased the length of flow separation (separation point moved upstream), but the reattachment point remained relatively constant.
3. The effect of decreasing the flap span when the flow was fully laminar, transitional, or fully turbulent was to decrease the plateau pressure and decrease the length of separation.

4. The fully laminar and transitional (transition near reattachment) plateau pressure coefficients correlated as $C_{pp} \sim (Re_{x_0})^{-1/4}$. The results obtained from an existing semi-empirical method were found to give a good prediction of the length of a fully laminar separated region.

REFERENCES

1. Anderson, A. "Flow Characteristics of a 12-in. Intermittent Supersonic Tunnel." AEDC-TDR-63-203, September 1963.
2. Test Facilities Handbook (5th Edition). "von Kármán Gas Dynamics Facility, Vol. 4." Arnold Engineering Development Center, July 1963.
3. Pate, S. R. and Brillhart, R. E. "Investigation of Boundary-Layer Transition on Swept Wings at Mach Numbers 2.5 to 5." AEDC-TDR-63-109, July 1963.
4. Potter, J. Leith and Whitfield, Jack D. "Effects of Unit Reynolds Number, Nose Bluntness, and Roughness on Boundary-Layer Transition." AEDC-TR-60-5, March 1960.
5. Galezowski, Stanley H. "Effects of Probe Tip Geometry and Size on Measurements in a Laminar Boundary Layer in Supersonic Flow." University of Toronto, UTIA TN-17, October 1957.
6. Davies, F. V. "Some Effects of Pitot Size on the Measurement of Boundary Layers in Supersonic Flow." Royal Aircraft Establishment (Great Britain) TN Aero 2179, August 1952.
7. Blue, Robert E. and Low, George M. "Factors Affecting Laminar Boundary Layer Measurements in a Supersonic Stream." NACA TN 2891, February 1953.
8. Chapman, Dean R., Kuehn, Donald M., and Larson, Howard K. "Investigation of Separated Flows in Supersonic and Subsonic Streams with Emphasis on the Effect of Transition." NACA Report 1356, 1958.
9. Kuehn, Donald M. "Experimental Investigation of the Pressure Rise Required for the Incipient Separation of Turbulent Boundary Layers in Two-Dimensional Supersonic Flow." NACA Memo 1-21-59A, February 1959.
10. Baer, A. L. "An Investigation of Separated Flows on Two-Dimensional Models at Mach Numbers 5 and 8." AEDC-TDR-63-200, September 1963.

11. Erdos, John and Pallone, Adrian. "Shock Boundary Layer Interaction and Flow Separation." RAD-TR-61-23, August 1961.
12. Hakkinen, R. J., Greber, I., Trilling, L., and Abarbanel, S. S. "The Interaction of an Oblique Shock Wave with a Laminar Boundary Layer." NACA Memo 2-18-59W, March 1959.
13. Van Driest, E. R. "Investigation of Laminar Boundary Layer in Compressible Fluids Using the Crocco Method." NACA TN 2597, January 1962.
14. Sterrett, J. R. and Emory, J. C. "Extension of Boundary Layer Separation Criteria to a Mach Number of 6.5 by Utilizing Flat Plates and Forward Facing Steps." NACA TN-D-618, December 1960.



Assembly

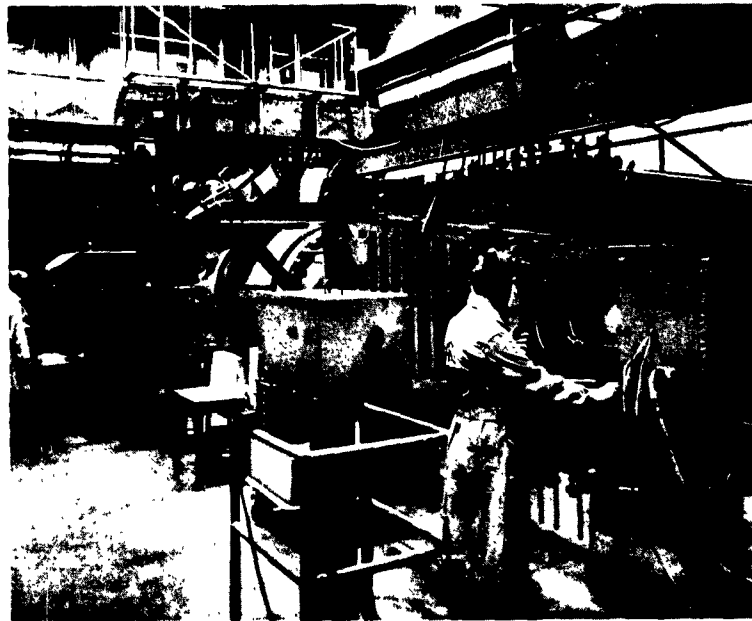
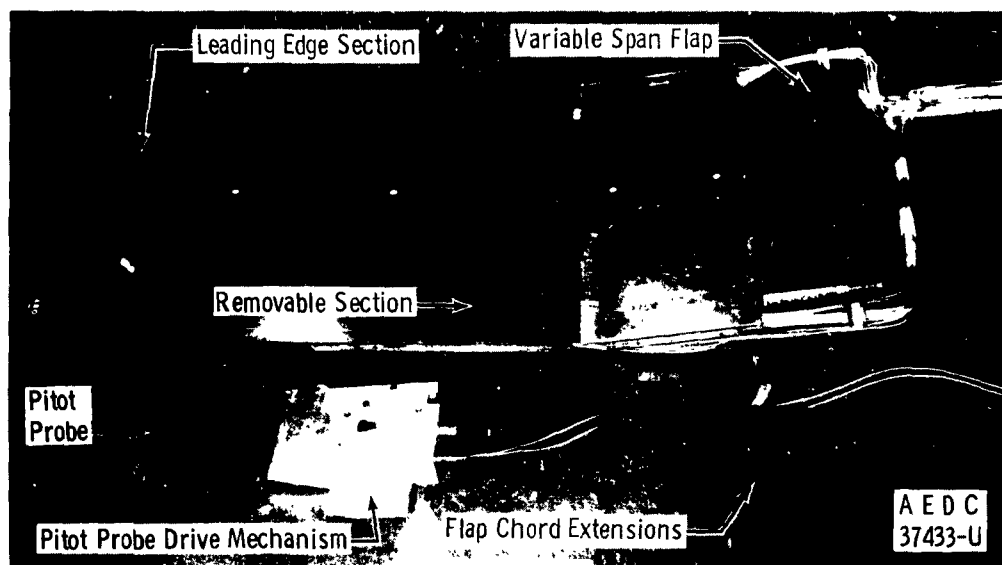
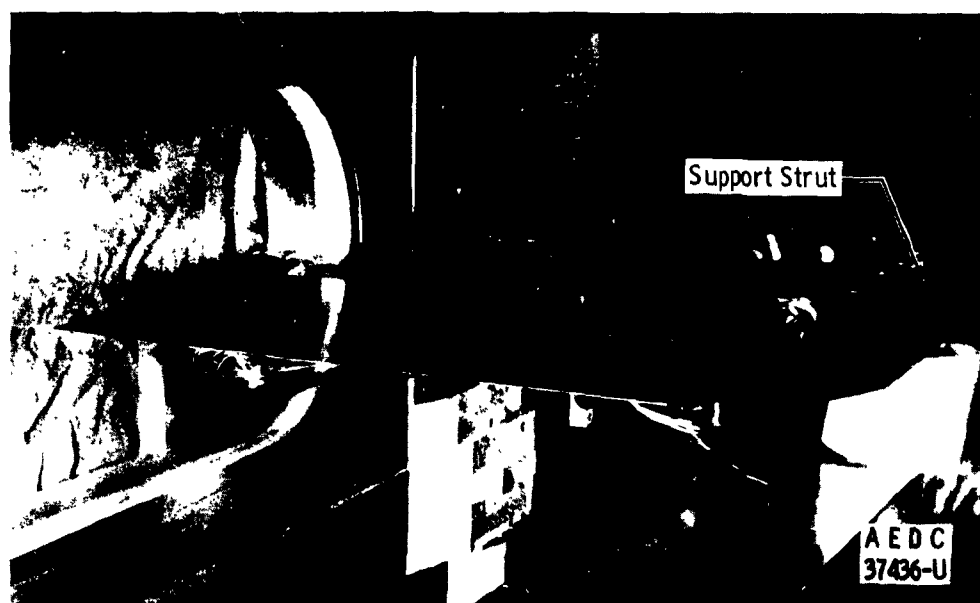


Fig. 1 Tunnel D



a. Model



b. Model Installation

Fig. 2 Model Photographs

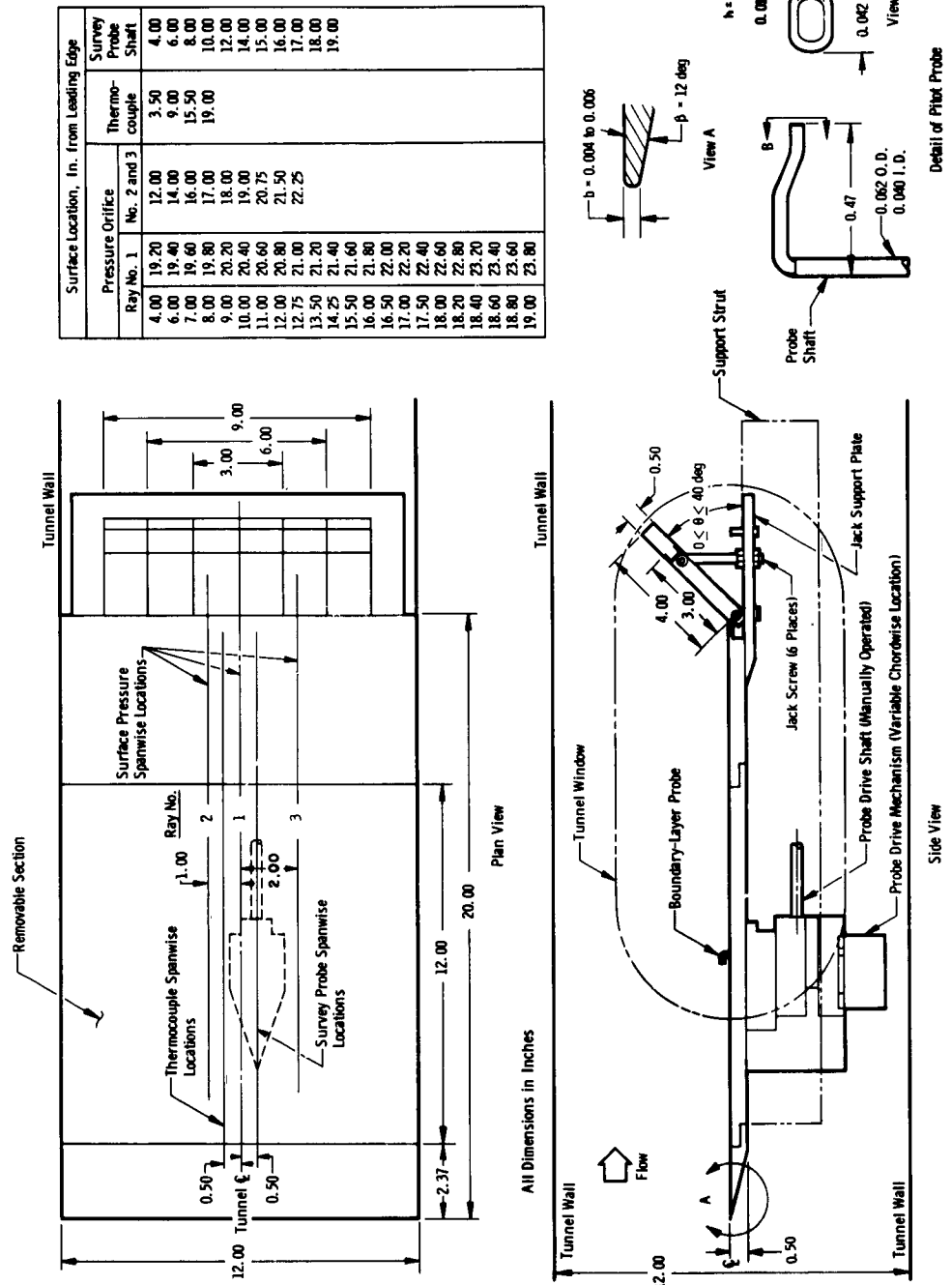
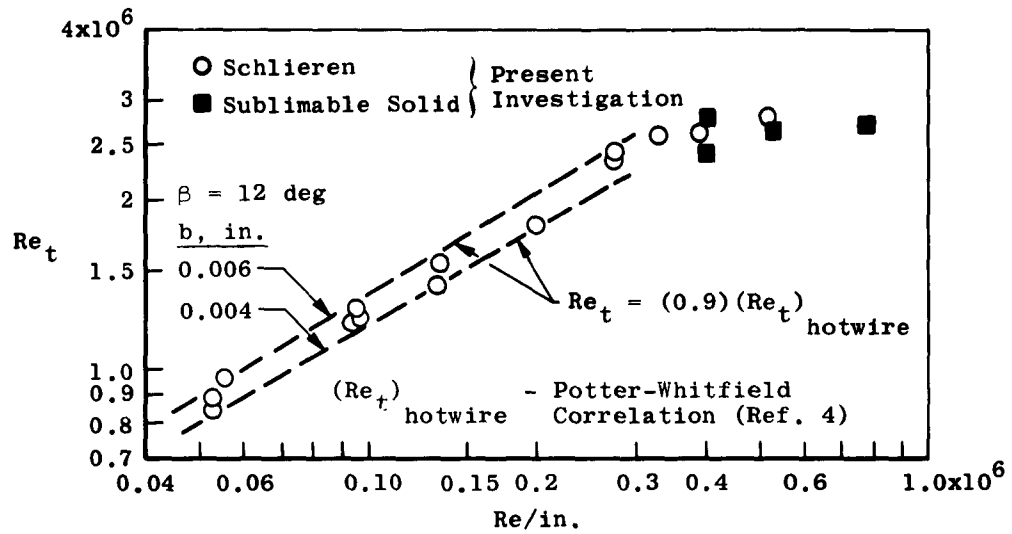
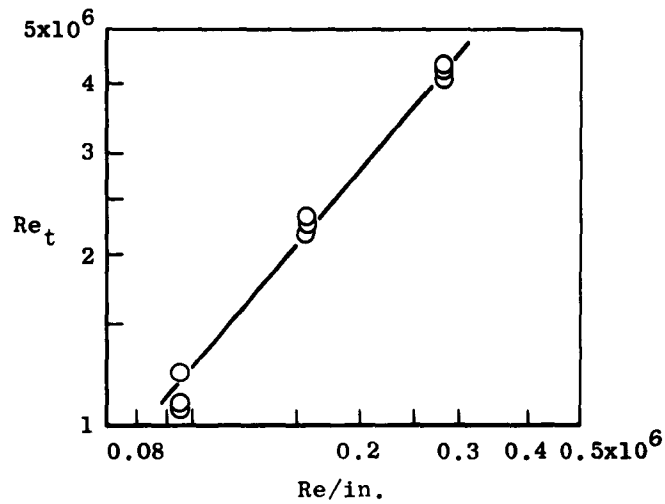


Fig. 3 Model Geometry

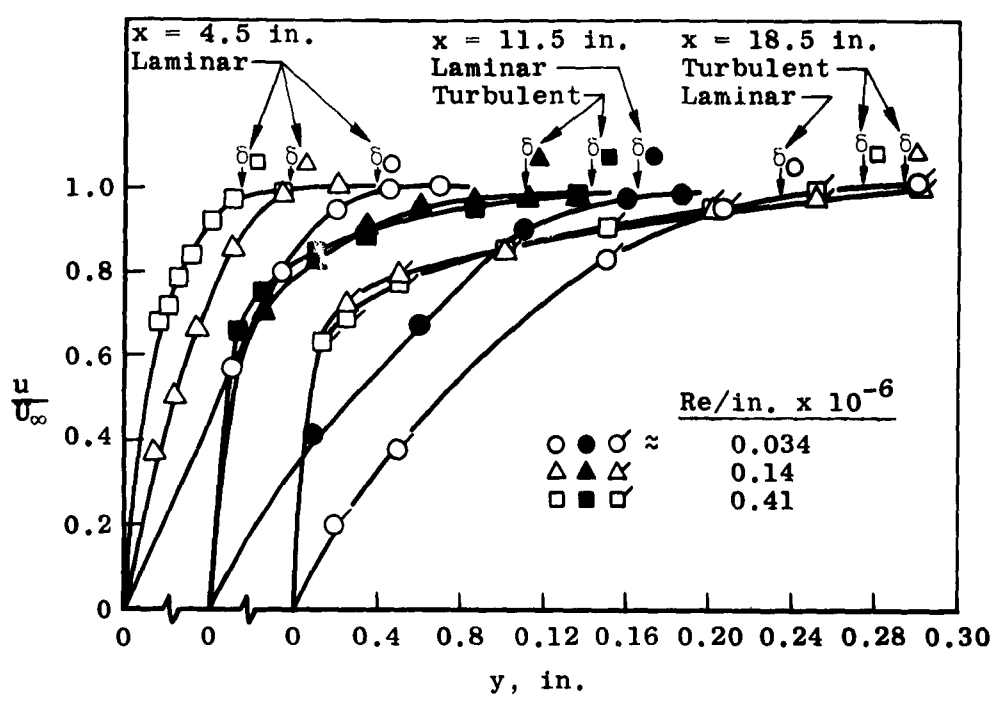


a. $M_\infty = 3$, Schlieren and Sublimable Solid Results

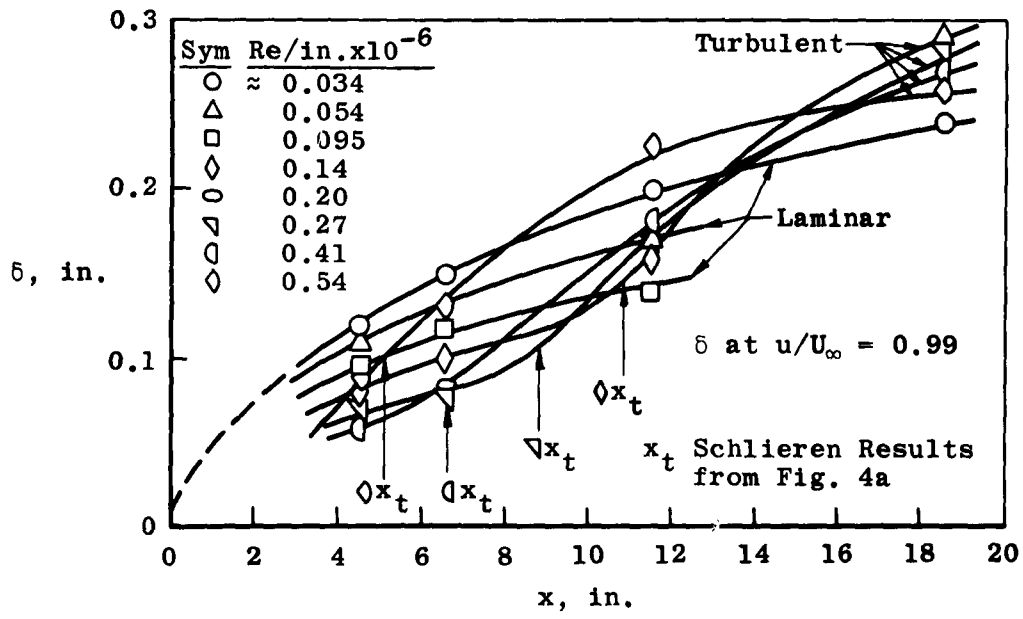


b. $M_\infty = 5$, Schlieren Results

Fig. 4 Boundary-Layer Transition Results at $M_\infty = 3$ and 5 for Zero Flap Deflection



a. Velocity Profiles at Various Model Stations

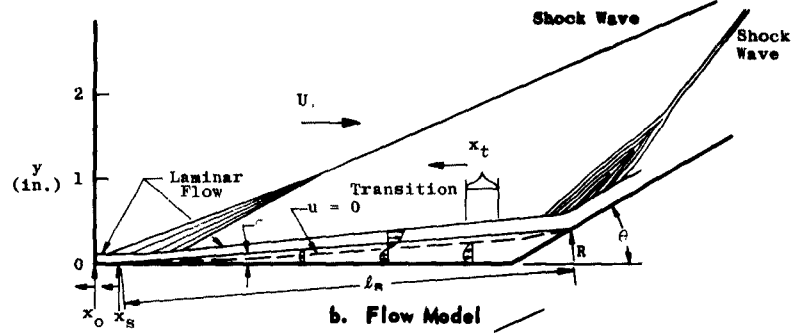


b. Boundary-Layer Growth

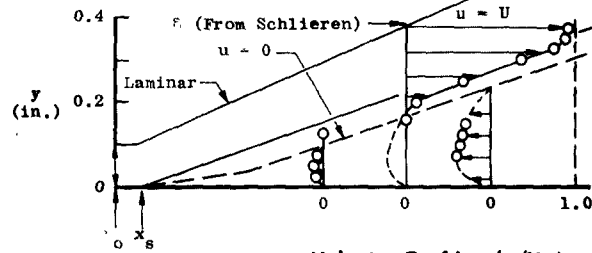
Fig. 5 Velocity Profiles and Boundary-Layer Thickness at Various Model Stations, $M_\infty = 3, \theta = 0$



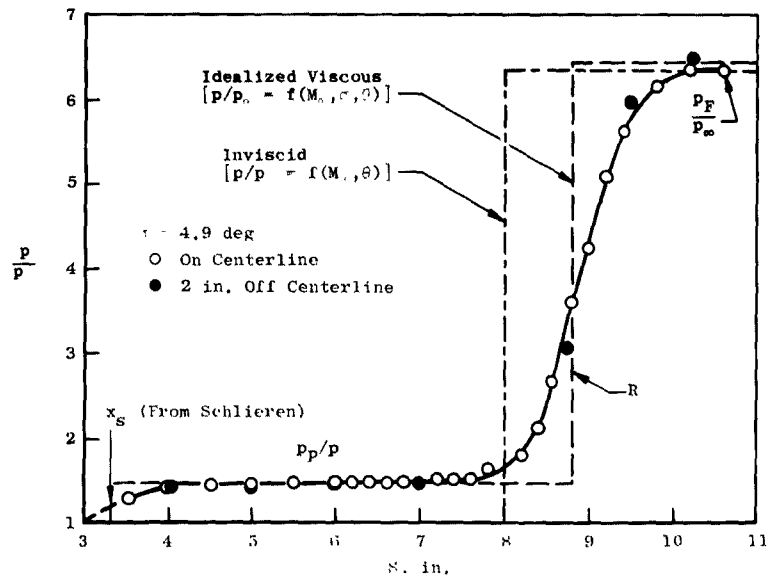
a. Schlieren Photograph



b. Flow Model



c. Velocity Profiles (u/U_∞)



d. Pressure Distribution

Fig. 6 Velocity Distributions and Surface Pressure Distribution at $M_\infty = 3$, $Re/in. = 0.036 \times 10^6$, $\theta = 30$ deg, Configuration 839



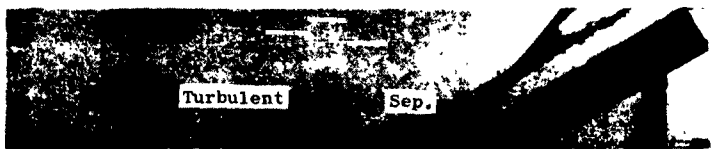
Re/in. = 0.097×10^6 , Sym \circ



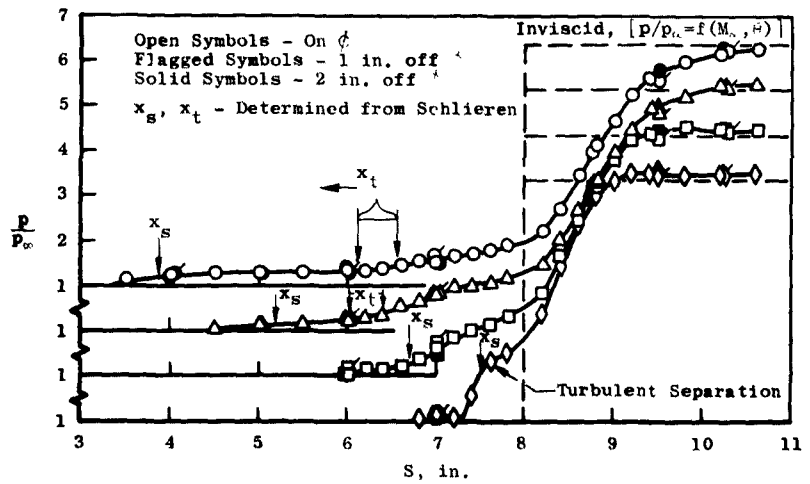
Re/in. = 0.21×10^6 , Sym \triangle



Re/in. = 0.28×10^6 , Sym \square

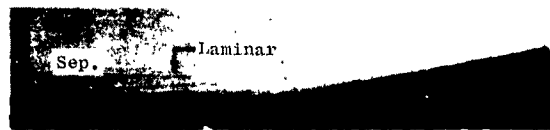


Re/in. = 0.42×10^6 , Sym \diamond



$\alpha. \theta = 30 \text{ deg}$

Fig. 7 Effect of Unit Reynolds Number on Surface Pressure Distribution and Separation, 8-in. Plate, $M_\infty = 3$, Configuration 839



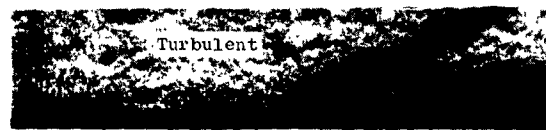
Re/in. = 0.034×10^6 , Sym \circ



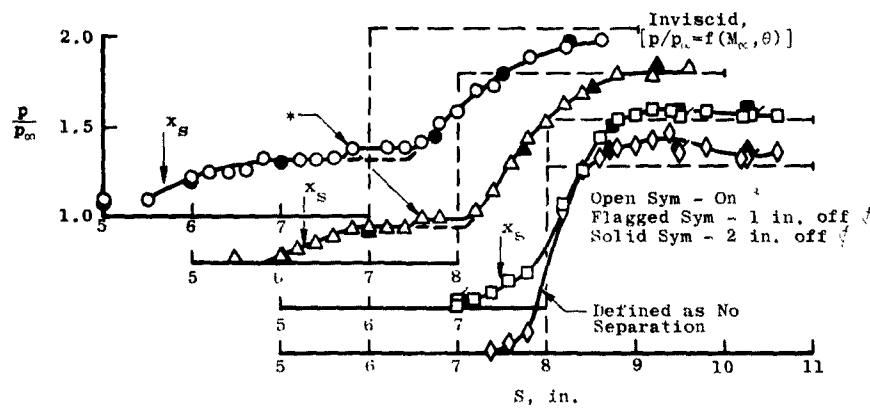
Re/in. = 0.094×10^6 , Sym \triangle



Re/in. = 0.20×10^6 , Sym \square



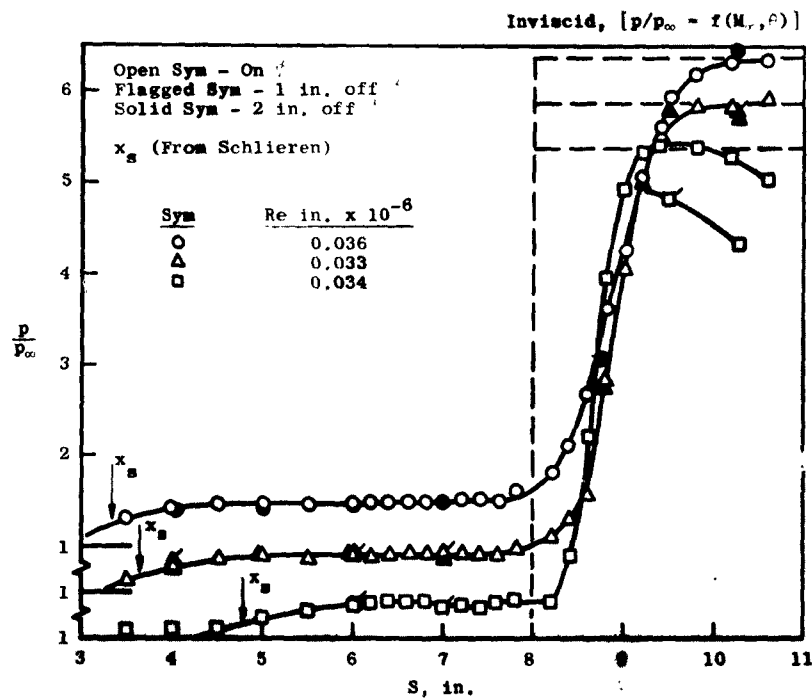
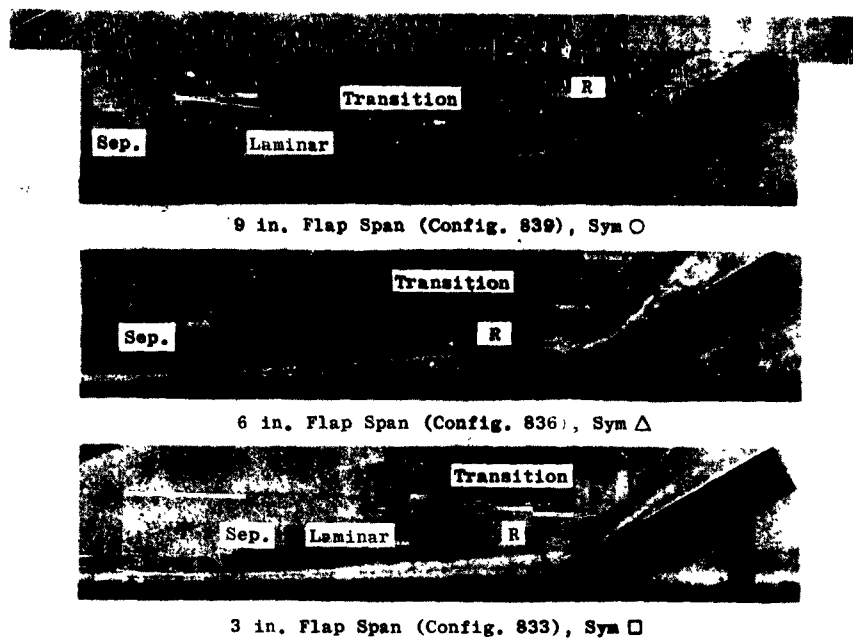
Re/in. = 0.26×10^6 , Sym \diamond



* Probably the result of a small amount of air leaking in between flap and model.

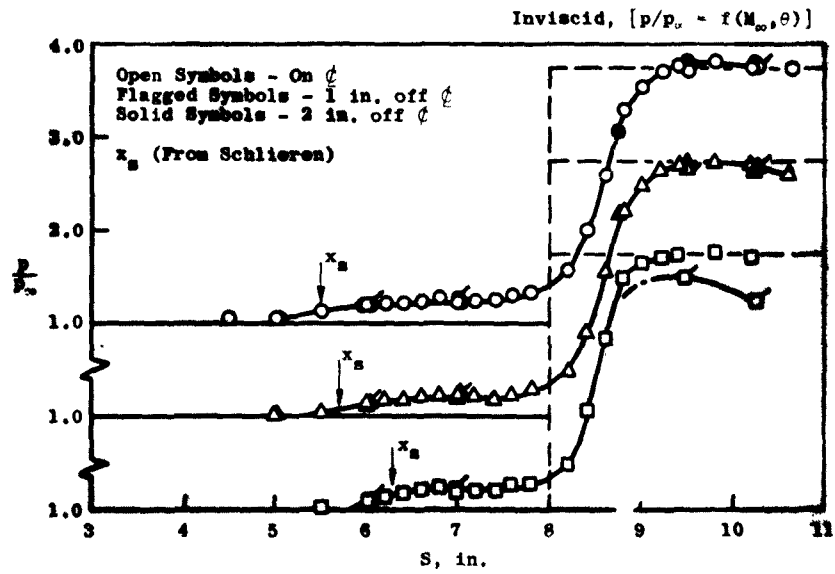
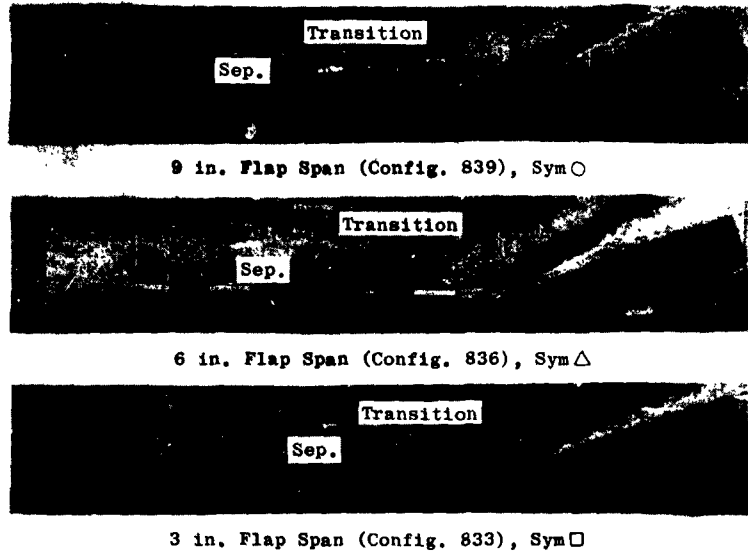
b. $\theta = 10$ deg

Fig. 7 Concluded



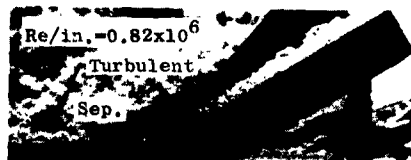
a. Flap Span Effect, $\theta = 30$ deg, $Re/in. = 0.034 \times 10^6$

Fig. 8 Flap Span and Unit Reynolds Number Effect, 8-in. Plate, $M_\infty = 3$



b. Flap Span Effect, $\theta = 20 \text{ deg}$, $Re/in. = 0.095 \times 10^6$

Fig. 8 Continued



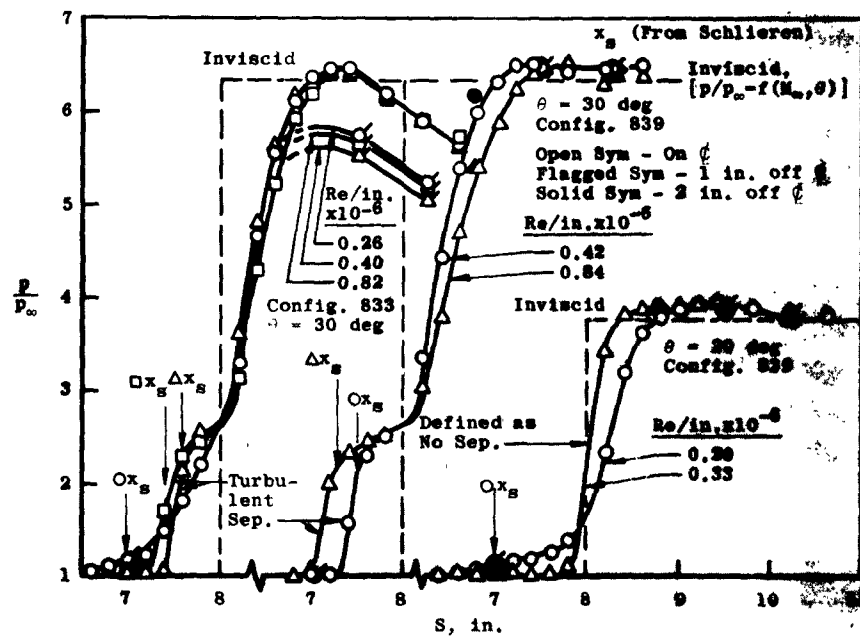
3 in. Flap Span (Config. 833), $\theta = 30$ deg



9 in. Flap Span (Config. 839), $\theta = 30$ deg



9 in. Flap Span (Config. 839), $\theta = 20$ deg



c. Flap Span and Reynolds Number Effect, $\theta = 30$ and 20 deg

Fig. 8 Concluded

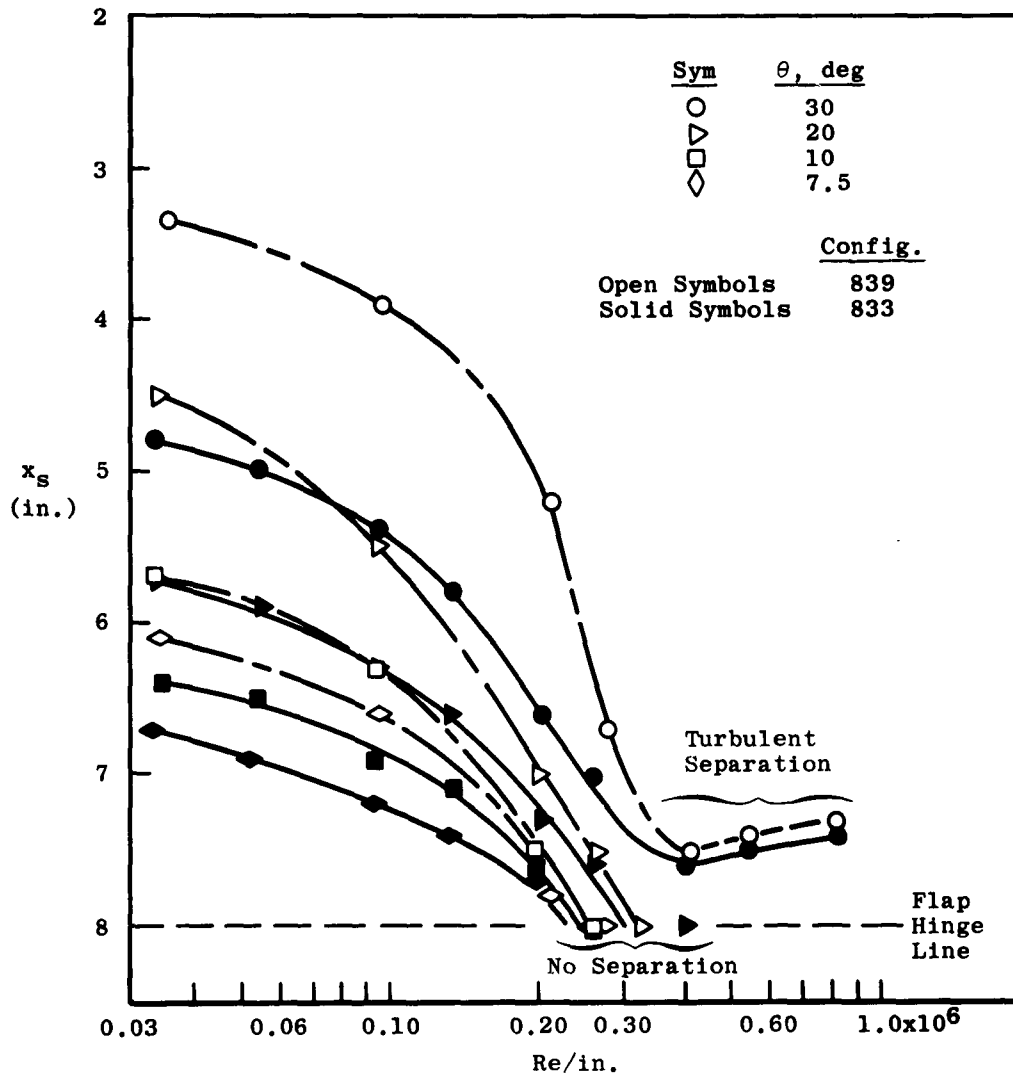
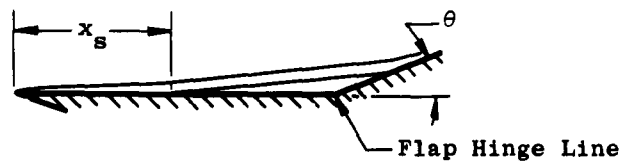


Fig. 9 Comparison of Separation Locations for Various Flap Angles and Flap Span Widths, 8-in. Plate, $M_\infty = 3$

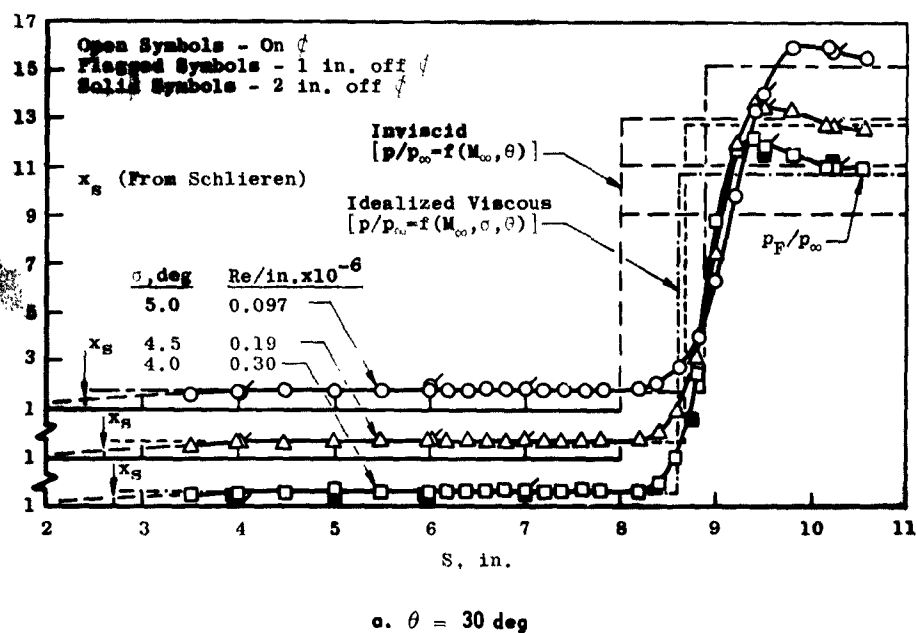
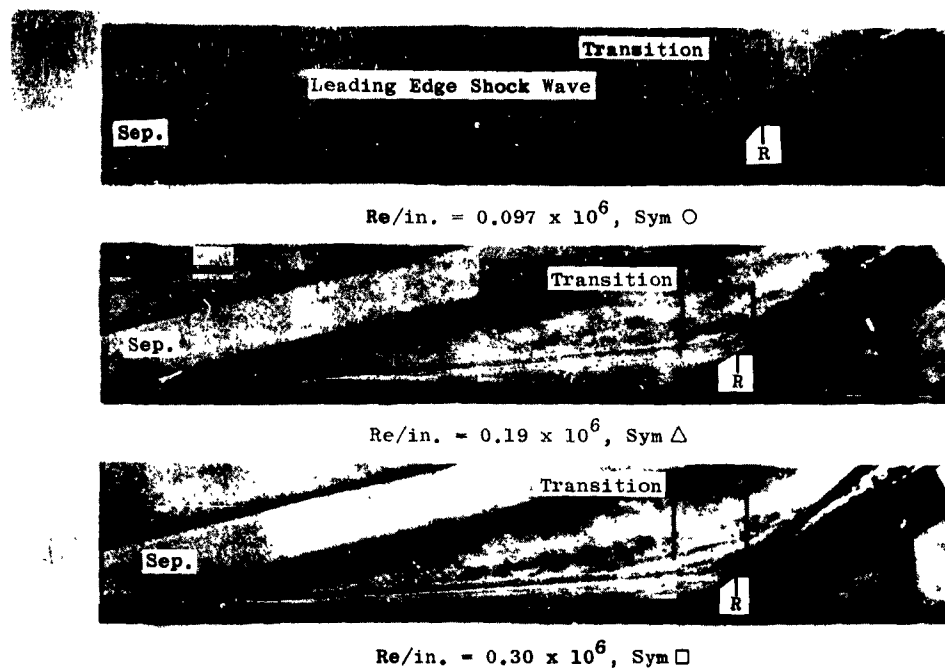
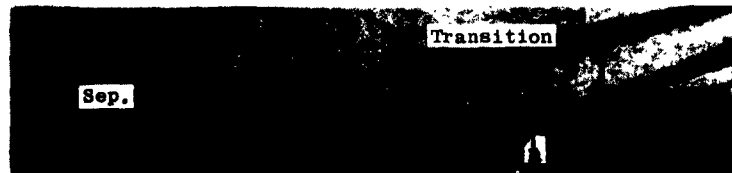


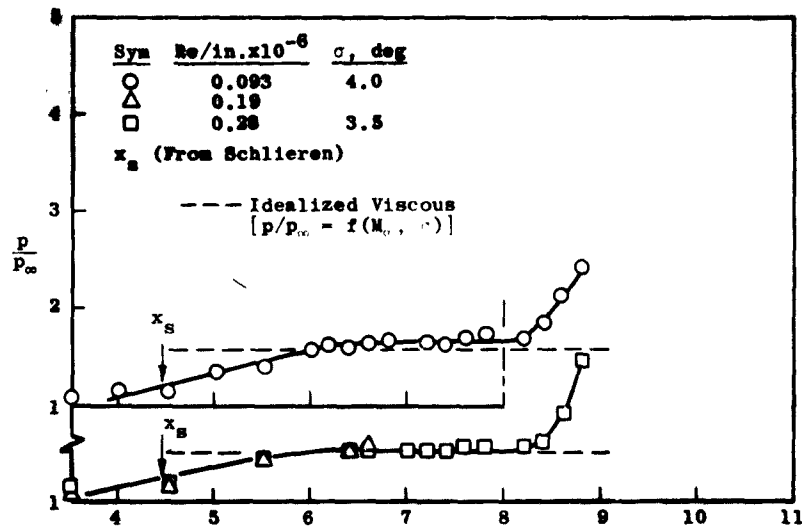
Fig. 11 The Effect of Unit Reynolds Number, 8-in Plate, $M_\infty = 5$, Configuration 839



Re/in. = 0.093×10^6 , Sym

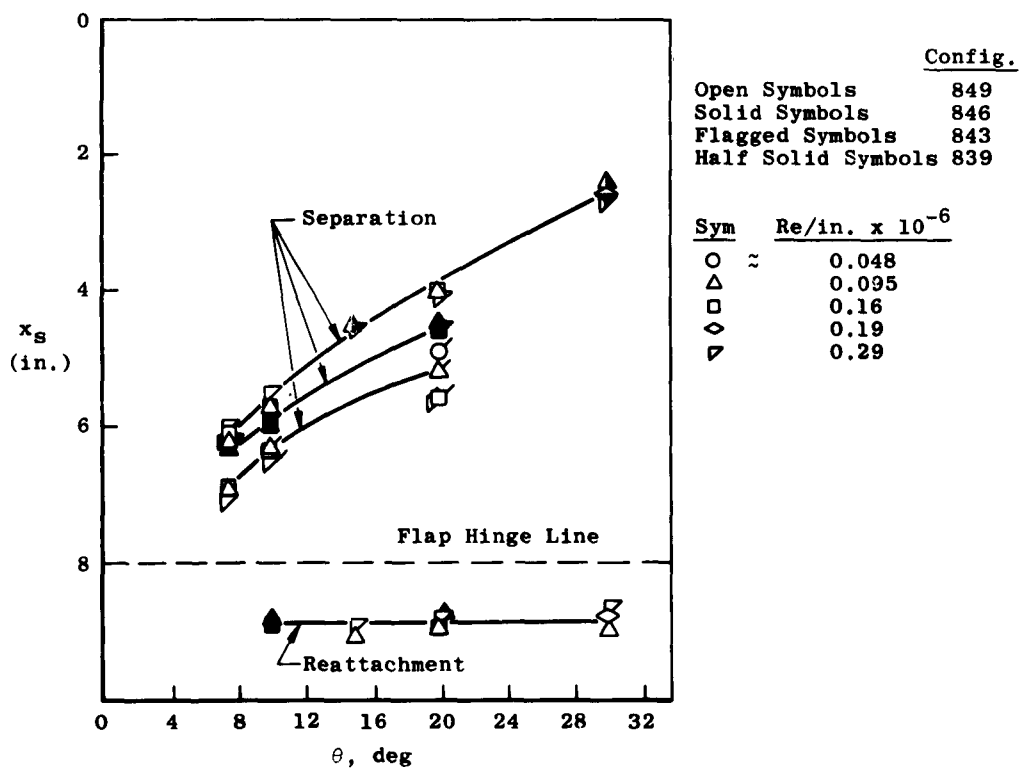
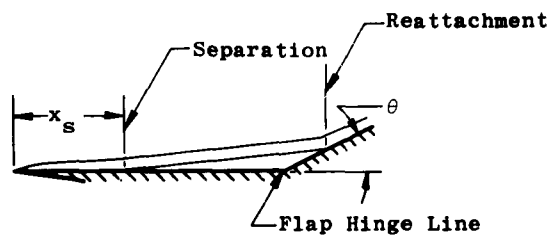


Re/in. = 0.28×10^6 , Sym



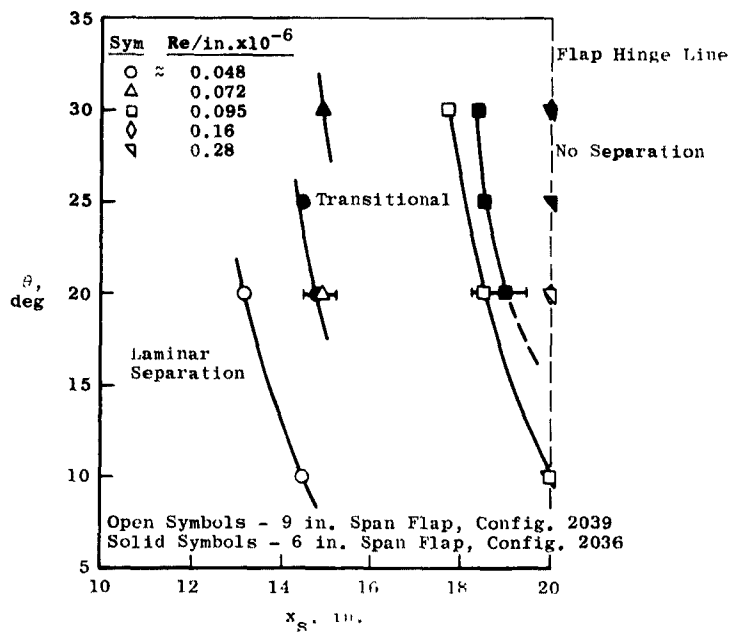
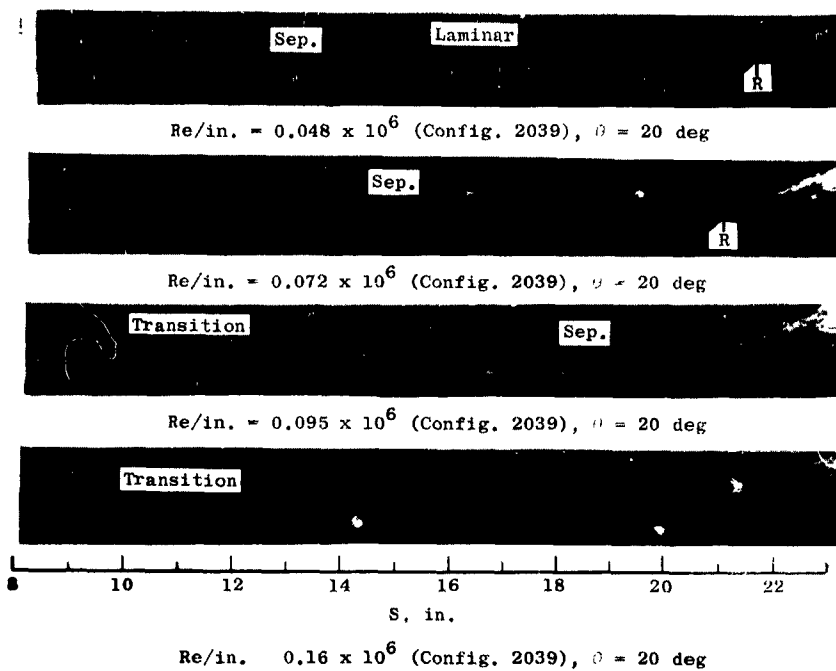
b. $\theta = 15$ deg

Fig. 11 Concluded



a. 8-in. Plate

Fig. 12 Variation in Separation Locations with Flap Deflection Angle (θ)
at $M_\infty = 5$

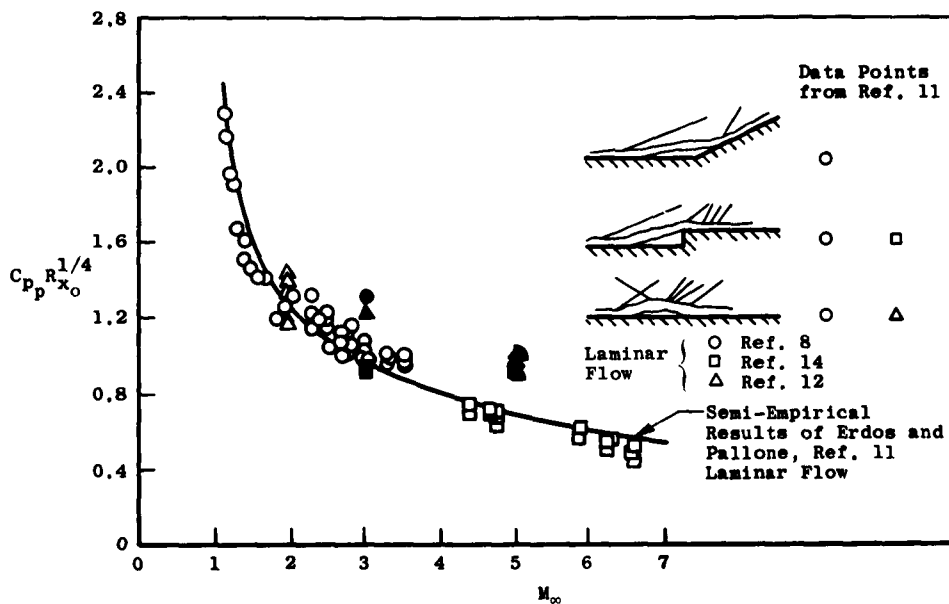


b. 20-in. Plate

Fig. 12 Concluded

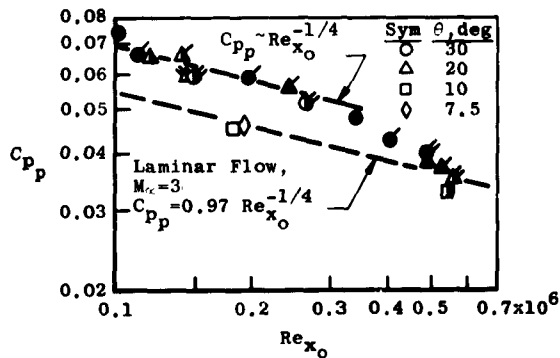
Config.	M_∞	$Re/in. \times 10^{-6}$	Sym	θ, deg	Remarks
839	3	0.035	●	30	Transition Upstream of Reattachment
3	3	0.034	▲	20	Transition in Reattachment Zone
3	3	0.034	■	10	Pure Laminar Separation
3	3	0.035	◻	7.5	Pure Laminar Separation
5	5	0.097 to 0.30	◆	30	Transition Upstream of Reattachment
5	5	0.093 to 0.28	■	15	Transition in Reattachment Zone

VKF-AEDC

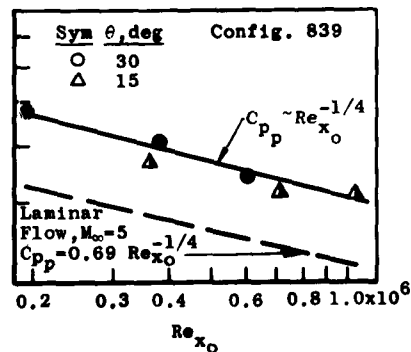


a. $M_\infty = 1$ to 7

	<u>Config.</u>	Solid Symbols - Transition Upstream of Reattachment
Unflagged	839	Half Solid Symbols - Transition in Reattachment Zone
Flagged	836	Open Symbols - Pure Laminar Flow
Double Flagged	833	--- Erdos and Pallone, Ref. 11



b. $M_\infty = 3$



c. $M_\infty = 5$

Fig. 13 Plateau Pressure for Laminar and Transitional Flow

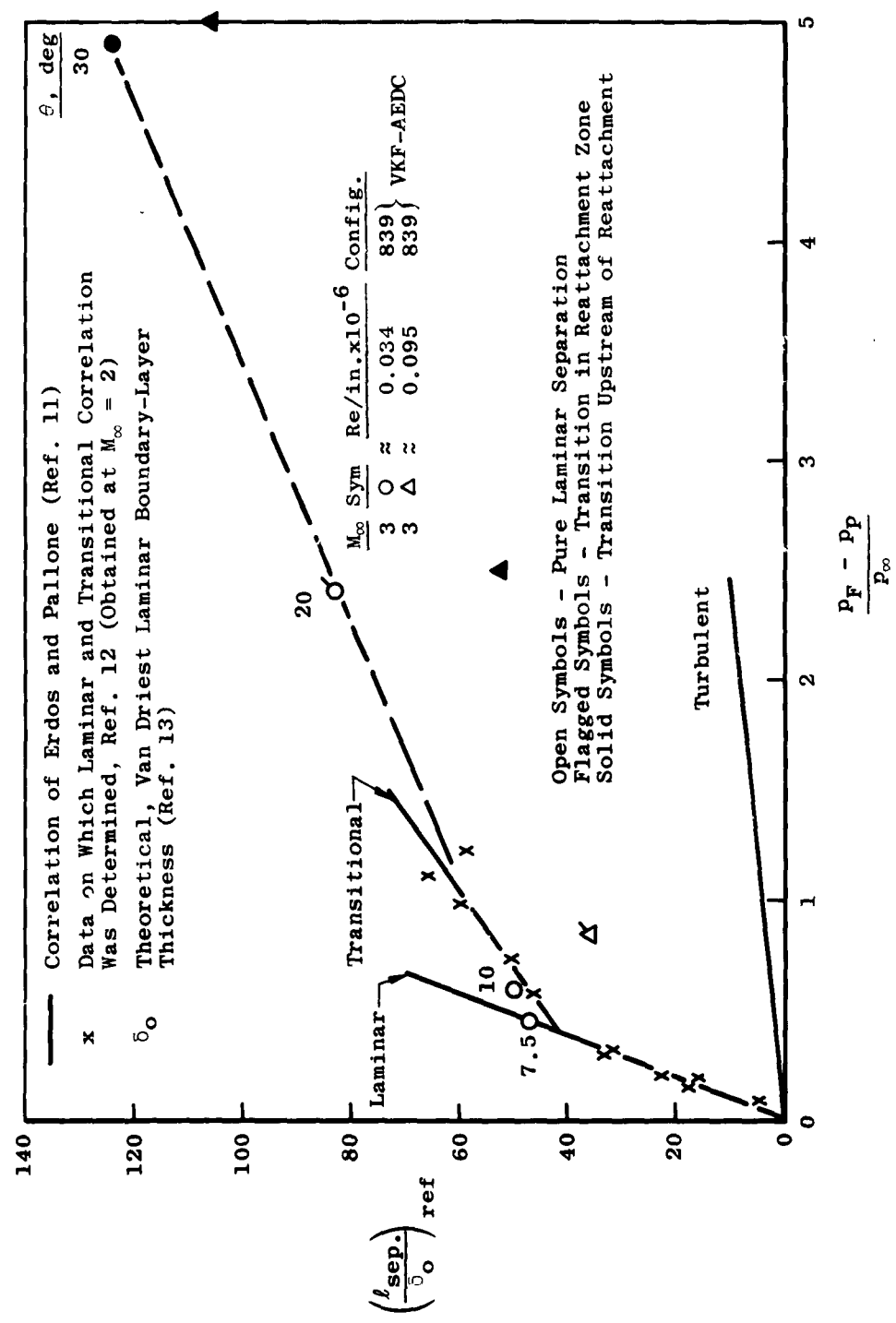
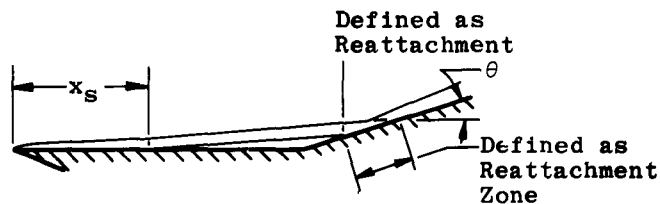


Fig. 14 Length of Laminar and Transitional Separation



Solid Symbols - Pure Laminar Separation
 Open Symbols - Transition in Reattachment Zone
 Flagged Symbols - Transition Upstream of Reattachment
 Half Solid Symbols - Transition Upstream of Separation
 (i.e. Turbulent Separation)

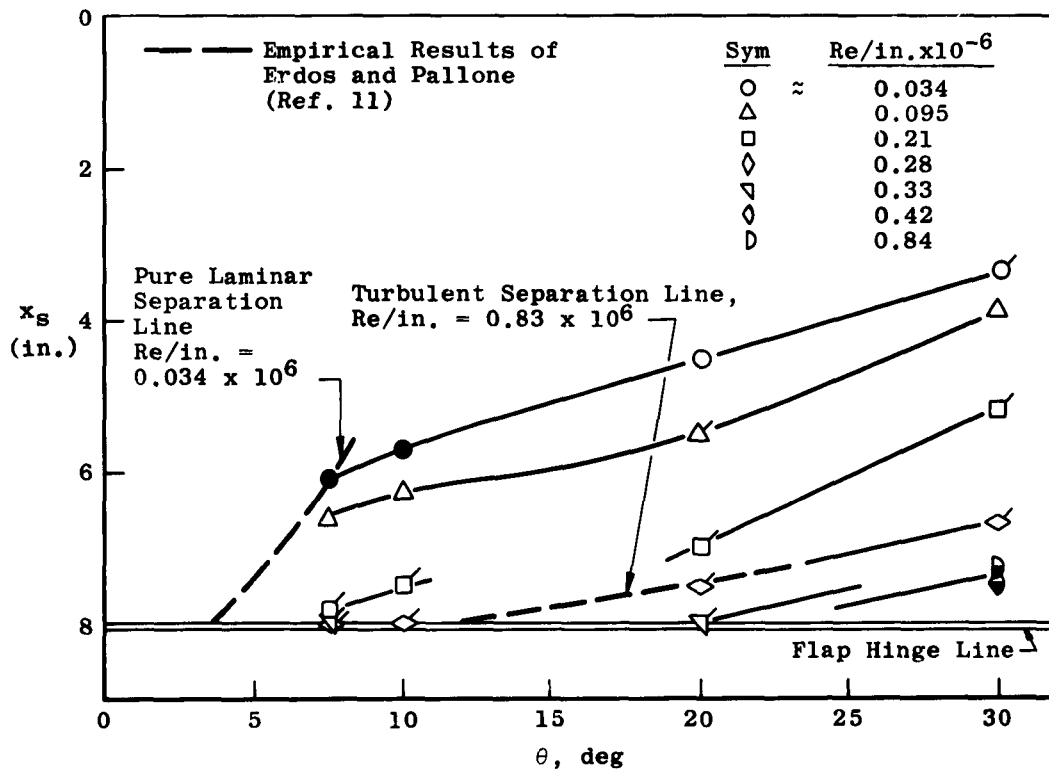


Fig. 15 Variation in Separation Location with Flap Deflection Angle (θ),
 $M_\infty = 3$, Configuration 839